Effect of carbon deposits on reactivity of supported Pd model catalysts

Sh.K. Shaikhutdinov [a,*], M. Frank [a], M. Bäumer [a], S.D. Jackson [b], R.J. Oldman [c], J.C. Hemminger [d], and H.-J. Freund [a]

[a] Fritz-Haber-Institut der Max-Planck-Gesellschaft, Faradayweg 4-6, Berlin 14195, Germany
[b] Department of Chemistry, University of Glasgow, Glasgow G12 8QQ, UK, and ICI Synetix, P.O. Box 1, Billingham, Cleveland TS23 1LB, UK
[c] ICI Technology, The Heath, Runcorn, Cheshire WA7 4QD, UK
[d] Department of Chemistry, University of California, Irvine CA 92697, USA

Received 4 December 2001; accepted 7 February 2002

Alumina-supported Pd model catalysts were prepared by Pd evaporation onto a thin alumina film grown on a NiAl(110) substrate. Adsorption and co-adsorption of ethene, CO and hydrogen on $Pd/Al_2O_3/NiAl(110)$ covered by carbon species, formed by ethene dehydrogenation at ~550 K, was studied by temperature programmed desorption (TPD). TPD results show that carbon deposits do not prevent adsorption but inhibit dehydrogenation of di-σ bonded ethene. Carbon species suppress CO adsorption in the highly coordinated sites and also suppress the formation of hydrogen ad-atoms on the surface. The ethene hydrogenation reaction performed by co-adsorption of hydrogen and ethene is inhibited by the presence of carbon deposits. The inhibition is independent of particle size studied (1–3 nm). The effects are rationalized in terms of a site-blocking behavior of carbon species occupying highly coordinated sites on the Pd surface.

KEY WORDS: ethene; carbon monoxide; hydrogen; hydrogenation; palladium; adsorption; particle size effect; temperature programmed desorption.

1. Introduction

The formation of various carbonaceous deposits during reactions of unsaturated hydrocarbons on metal catalysts is well established. Over the years, there has been continuing interest in examining the nature of these species and their role in catalysis. It has turned out that carbon deposits may exhibit poisoning effects, whereas carbonaceous and hydrocarbonaceous deposits show beneficial effects in terms of influencing the catalytic behavior on the surface (*e.g.*, see [1]).

In the past few years, we have shown that metal particles deposited on a thin well-ordered alumina film grown on a NiAl(110) single crystal are very suitable model systems for studying structure–activity relationships in catalysis, particularly in CO oxidation and ethene hydrogenation reactions [2–6]. For example, the adsorption properties of the $Pd/Al_2O_3/NiAl(110)$ surface toward ethene and hydrogen gradually change as a function of particle size. However, the activity of this system for the ethene hydrogenation reaction observed in co-adsorption experiments is independent of the particle size, in agreement with the general opinion in the literature regarding structural insensitivity of hydrogenation reactions [6].

The interaction of this system with CO/O_2 turns out to be more complicated: oxygen exposure at 400–500 K (oxidation) results in increasing oxide film thickness due to the Pd-catalyzed oxidation of the metallic substrate underneath the oxide layer [7]. However, after removing oxygen from the Pd surface by its reaction with CO (reduction), the adsorption–desorption properties of Pd particles are very similar to those of the pristine system. The resulting Pd/alumina system has a high thermal stability and resembles real catalysts supported on bulk oxide substrates. Also, this procedure somewhat mimics the preparation of real catalysts involving calcination and reduction steps. Accordingly, we use the oxidation–reduction treatments mentioned above for the preparation of the Pd/alumina model catalysts.

In order to rationalize effects of carbon deposits on catalytic properties of small metal particles, it is necessary to study the influence of carbon species on the individual adsorption of molecules participating in reactions, typically CO, hydrogen and hydrocarbons. In the present paper, we employed temperature programmed desorption (TPD) for studying adsorption and the ethene hydrogenation reaction on Pd/alumina model catalysts in the presence of carbon residues.

2. Experimental

The experiments were performed in an ultra-high vacuum (UHV) chamber (base pressure below 10^{-10} mbar). A NiAl(110) single crystal of $8 \times 10 \times 1\,mm^3$ was spot-welded to two parallel Ta wires for

* To whom correspondence should be addressed.

1011-372X/02/0600-0115/0

resistive heating. Cooling down to ~80 K was achieved by filling a manipulator rod with liquid nitrogen. The temperature was measured by a chromel–alumel thermocouple spot-welded to the back side of the crystal and controlled by using a feedback system (Schlichting Physical Instruments).

The quadrupole mass spectrometer (QMS, Fisons) had a differentially pumped shield. For the TPD measurements, the sample was placed about 0.5 mm in front of the nozzle of the shield to ensure that the signal was coming from the sample surface only. The computer-multiplexed mass spectrometer allowed up to 16 masses to be simultaneously monitored.

All gas exposures were performed with a directional doser. D_2 (99.9%, isotopic content 99.5%), O_2 (99.999%) and CO (99.999%) were supplied by AGA Gas GmbH, and ethene C_2D_4 (99.9%, isotope content 99%) by Isotec Inc.

The thin alumina film was prepared by two cycles of oxidation of the clean NiAl(110) surface in 10^{-6} mbar of O_2 at 550 K and annealing at ~1130 K for 4–5 min. Palladium (99.99%, Goodfellow) was deposited onto the alumina film using a commercial evaporator (Focus EFM 3). Note that with this kind of evaporator, the sample must be biased with a retarding potential in order to prevent metal ions from being accelerated toward the sample and creating nucleation centers on the surface. Typical Pd deposition rates were about 0.7 Å min^{-1}, as calibrated with a quartz microbalance.

Palladium was deposited onto the alumina film kept at ~90 K. Then the sample was exposed to 500 L of O_2 (1 L = 10^{-6} Torr sec) at 500 K followed by exposure to 4 L of CO at 300 K and heating to 600 K to desorb CO and CO_2 [7]. The resulting Pd surfaces showed reproducible CO and D_2 TPD spectra, thus indicating that no further morphological changes occur during TPD measurements.

The mean Pd particle size was determined based on a combined scanning tunneling microscopy (STM) and microbalance study assuming a hemispherical particle shape. The corresponding relationship between particle size and nominal thickness has been presented in reference [6].

X-ray photoelectron spectroscopy (XPS) measurements were performed using a Mg K_α X-ray source (Fisons) and a hemispherical analyzer (Scienta SES 200).

3. Results and discussions

3.1. Carbon deposition

Previous vibrational spectroscopy studies on Pd single crystal surfaces have shown that ethene dehydrogenates on Pd and forms several stable intermediate species depending on metal surface symmetry, temperature and coverage [8–10]. Finally, a carbon overlayer is suggested to form at elevated temperatures. On supported Pd particles, it is difficult to assign precisely the steps of ethene dehydrogenation. We have previously observed formation of ethylidyne ($\equiv C-CH_3$) species, characteristic for the Pd(111) surface, by infrared reflection absorption spectroscopy (IRAS) on the largest (~4 nm) particles at 250–300 K [3,5]. This finding indicates that large particles mainly expose (111) facets, in agreement with STM observations [2].

Carbon deposition has been monitored by XPS. Figure 1 shows the C 1s region of XP spectra obtained for a Pd overlayer of 6.5 Å nominal thickness, with a mean particle size of ~4 nm.

At 90 K, ethene is mostly adsorbed *via* a π-bond, and no dehydrogenation occurs at these temperatures [5,11]. Therefore, the observed signal with a binding energy (BE) of 283.6 eV is assigned to molecular ethene.

On heating to room temperature, ethene preferentially desorbs intact [6]. However, a small fraction dehydrogenates and converts into adsorbed species such as ethylidyne [5]. These species exhibit a relatively broad C 1s signal with a BE of 283.3 eV. After annealing at 730 K, peak intensity is retained but it shifts to ~283.8 eV due to formation of other carbon species in the course of further dehydrogenation steps.

However, precise assignment of the carbon species (*e.g.* carbidic, graphitic) formed on Pd particles on heating to elevated temperatures is quite difficult from these XPS spectra.

The dehydrogenation reaction leads to hydrogen evolution detected in multimass TPD spectra. Typically, the H_2 (or D_2) signal exhibits a main β_2 peak at ~320 K and, depending on the particle size, either well-resolved γ peaks or a shoulder extending to ~500 K ([6] and see, for example, figure 2(b)). No hydrogen signal is detected at higher temperatures. This means that ethene completely decomposes on heating to $T > 500$ K and forms a

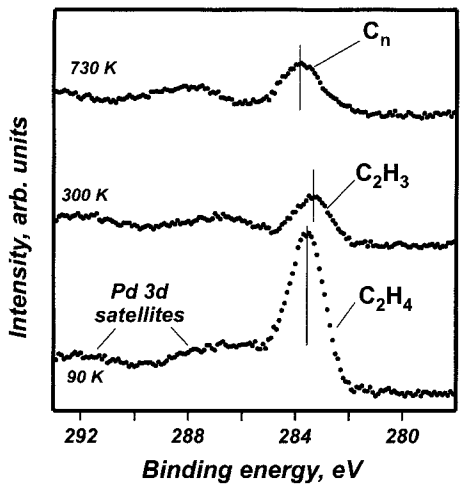

Figure 1. C 1s region of XP spectra obtained for 4 nm particles, deposited at 90 K, after saturation exposure to C_2H_4 at 90 K and subsequent heating to 300 K and 730 K.

carbon overlayer on the metal surface. However, small amounts of hydrogen-deficient CH_x species still remaining on the surface cannot be excluded.

Nevertheless, in order to record all desorbing products by TPD, the samples must be heated up to at least ~550 K. Therefore, with TPD it seems possible to study only the effects of the carbon species formed at final temperatures of 550–600 K. Otherwise, if dehydrogenated C_xH_y species were pre-formed on the Pd surface at a lower temperature, their own thermal transformations would interfere with desorption processes of newly adsorbed molecules and hence result in much more complex TPD spectra. Therefore, in the present study, we have focused on the effects of carbon deposits formed by exposure to saturating amounts of ethene at 90–100 K and subsequent heating to 550–600 K.

3.2. *Effect of carbon species on ethene adsorption*

TPD spectra of ethene at saturation exposure for the clean Pd particles exhibit a broad signal between the adsorption temperature and ~400 K. Based on a combined IRAS and TPD study, we have previously assigned ethene desorbing at $T < 250$ K to the weakly adsorbed molecules coordinated to Pd surface atom *via* a π-bond [3,5,6]. On the other hand, a desorption peak around 300 K, which dominates for the largest particles, has been attributed to the desorption of di-σ-bonded ethene.

Figure 2 presents a series of consecutive TPD spectra obtained after adsorption of 1 L of C_2D_4 at 100 K in each case. The traces of C_2D_4 (32 amu) and D_2 (4 amu) have been simultaneously recorded.

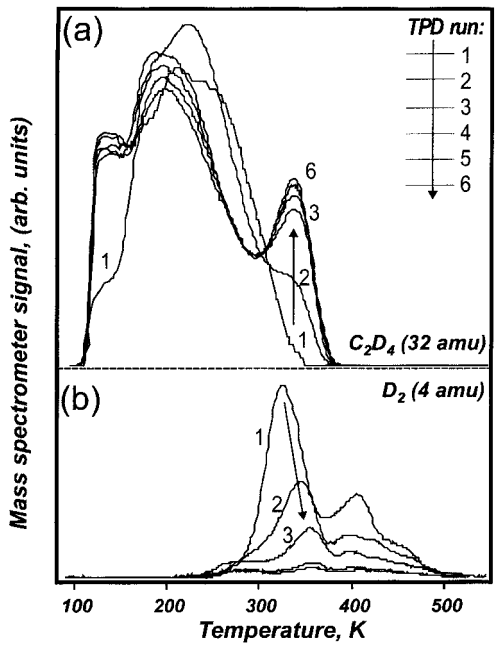

Figure 2. Consecutive TPD spectra obtained for adsorption of 1 L of C_2D_4 at 100 K after each run to 550 K. Panels (a) and (b) show simultaneous spectra for C_2D_4 and D_2, respectively. The contribution of the ethene cracking pattern to the 4 amu signal has been subtracted. The mean particle size is 2.5 nm.

Figure 2(b) shows that the D_2 signal is most intense for the clean Pd particles (first run). Its intensity gradually vanishes with increasing number of ethene adsorption/desorption cycles. This means that dehydrogenation activity of the Pd particles decreases as carbon deposits are accumulated in the previous cycles.

Meanwhile, the ethene desorption signal at ~200 K changes only to a minor extent, thus indicating that weakly bonded ethene is only slightly influenced by carbon deposits. In contrast, the signal at ~330 K grows with increasing cycle number. These data clearly show an inverse relation between ethene desorption at $T > 300$ K and hydrogen evolution. (Such a behavior has been observed for all samples studied, independent of Pd particle size.) Therefore, we can conclude that carbon species on the Pd surface do not prevent ethene *adsorption* but suppress the *dehydrogenation* reaction of strongly bonded (*i.e.* di-σ-bonded) ethene molecules.

The above results can be readily understood in terms of a previously suggested scheme [6] for the thermal transformation of ethene adsorbed on Pd particles, as shown below:

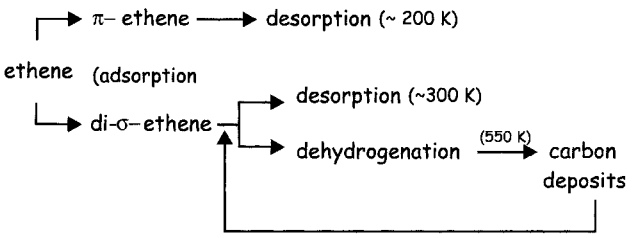

At low temperatures, ethene adsorbs in π- or di-σ-geometry. On heating, π-bonded ethene desorbs intact, while di-σ-bonded ethene can either desorb or dehydrogenate, thus producing carbonaceous species. Carbon species formed in the first TPD cycle inhibit the dehydrogenation reaction and favor ethene desorption in the second TPD cycle. In the next adsorption/desorption cycles, the active sites responsible for dehydrogenation are continuously occupied by carbon species. Finally, after 3–4 cycles, the system exhibits only ethene desorption since all sites for dehydrogenation are blocked by carbon deposits.

It seems plausible that carbon species, at least at low coverage, occupy highly coordinated sites on the metal surface such as 4-fold and 3-fold hollow sites on (100) and (111) surfaces, respectively (*e.g.* [12,13]). This could explain the small effect on the weakly bonded (π-) ethene molecules (see figure 1) which adsorb on the on-top sites. In contrast, the effect is much stronger for thermal transformation of di-σ-bonded ethene, since its dehydrogenation on Pd(111) facets proceeds via formation of the ethylidyne species coordinated to three Pd atoms in 3-fold hollow sites. However, these sites become occupied by carbon species in the course of carbon deposition.

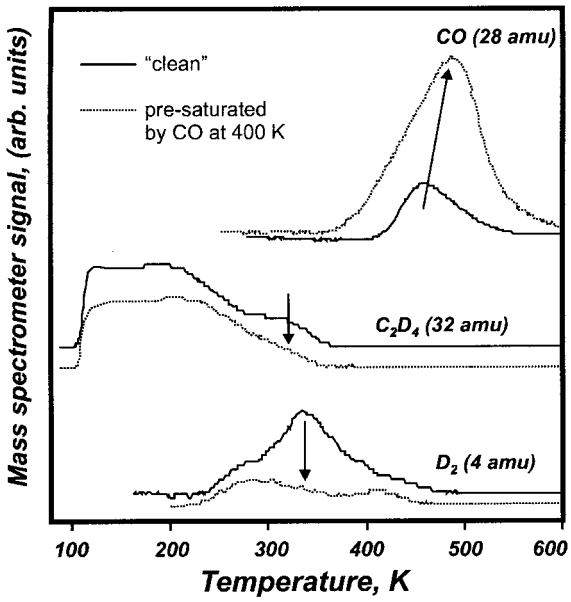

Figure 3. Multimass TPD spectra obtained after adsorption of 1 L of C_2D_4 at 100 K on the clean and CO pre-exposed 1.5 nm Pd particles. The contributions of the ethene cracking pattern to the 4 and 28 amu signals have been subtracted. The arrows highlight the differences between the spectra.

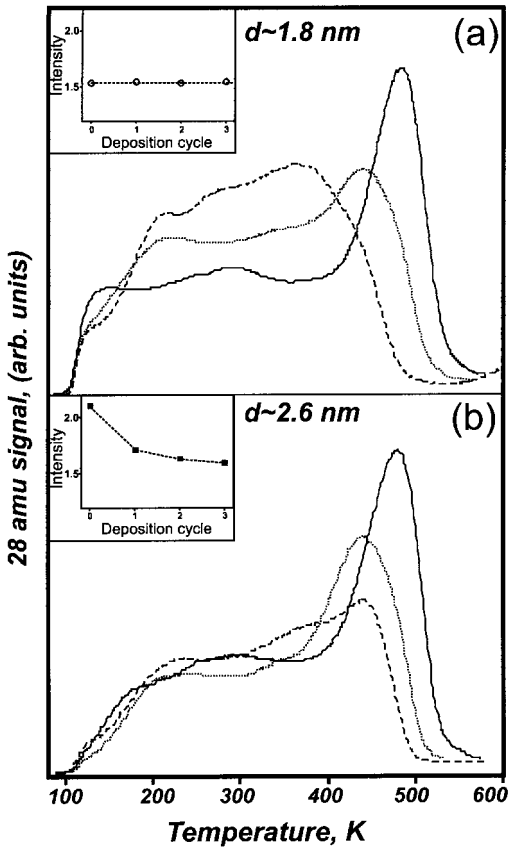

Figure 4. CO TPD spectra obtained by adsorption of 1 L of CO at 100 K on Pd particles of 1.8 nm (a) and 2.6 nm (b) in size. Shown are TPD spectra for the clean surfaces (—), after one (···) and three (---) carbon deposition cycles (1 L of C_2D_4 at 100 K and heating to 580 K). The insets show the desorption signal area as a function of cycle number.

In order to look further at site-specific ethene adsorption, we have performed ethene adsorption on a CO pre-covered Pd surface. The idea is that, at low coverage, CO occupies highly coordinated sites; therefore, we expect pre-adsorbed CO molecules to affect di-σ-ethene adsorption on these sites.

Figure 3 shows multi-mass TPD spectra obtained after ethene adsorption on clean and CO pre-covered Pd particles. Note that the "clean" Pd surface has in fact adsorbed small amounts of CO from the vacuum background. Nevertheless, comparing the spectra, we see that the amount of ethene desorbing at $T < 250$ K is independent of CO, thus indicating that π-bonded ethene is not affected by CO adsorbing in highly coordinated sites.

Meanwhile, the C_2D_4 desorption signal at temperatures above 300 K, as well as the D_2 signal corresponding to the dehydrogenation reaction, is suppressed by CO pre-adsorption. Therefore, data again show a correlation between the formation of di-σ-bonded ethene and ethene dehydrogenation. This means that it is di-σ-bonded ethene which dehydrogenates on the Pd particles, in agreement with the general opinion in the literature [11].

3.3. CO adsorption on carbon-covered Pd

The experiments were performed as follows. After the first CO TPD cycle on the freshly prepared sample, the Pd particles were exposed to 1 L of C_2D_4 at 100 K and heated up to ~580 K for the carbon deposition. Then, the sample was again exposed to 1 L of CO at 100 K. On heating, no other desorbing molecules were detected in the TPD spectra apart from CO. The spectra could be reproduced many times, thus indicating that CO does not react with the carbon species produced by ethene decomposition. Based on IRAS studies [2,3], it is known that CO may adsorb on on-top sites (linear CO), bridge and 3-fold hollow sites (multiply bonded CO) with different adsorption energies. These species relate to the different desorption temperatures in TPD spectra for Pd particles [2,7]. This allows us to monitor the distribution of adsorption sites accessible for CO on the carbon-covered Pd surface.

Figure 4 shows a series of CO TPD spectra obtained for (a) 1.8 nm and (b) 2.6 nm Pd particles. The spectra reveal that the carbon species strongly influence CO post-adsorption. As shown in (a), the main high temperature (HT) desorption peak at ~485 K obtained for the clean surface is shifted by ~45 K to lower temperature and decreases by ~30% in amplitude after the first carbon deposition cycle. In contrast, the broad low temperature (LT) desorption signal gains intensity. The signal shape gradually changes, with the original HT peak vanishing after three TPD cycles.

The overall effect depends on particle size. As shown in the spectra for the 2.6 nm particles (figure 4(b)), the

peak at ~480 K again shifts to ~440 K after the first deposition cycle, and its amplitude decreases with increasing amounts of carbon deposited. However, the LT region of the spectra does not change markedly, in contrast to the case of the 1.8 nm particles. In addition, the integral CO desorption area decreases with the cycle number for the 2.6 nm particles, but it remains constant for the smaller (1.8 nm) particles, as shown in the insets in figure 4.

In order to explain the observed changes in the CO TPD spectra induced by carbon residues, we have to recall here the assignment of TPD signals for CO on Pd particles [2,7]. At saturation exposure and at low temperatures, CO adsorbs on on-top sites as well as on multiply coordinated sites. On heating, CO desorbs from the more weakly held on-top sites resulting in a broad LT signal at $T \approx 100$–300 K. As the coverage decreases, the remaining CO molecules occupy energetically more favorable bridge and 3-fold hollow sites, and then desorb at a higher temperature. The HT peak is typically centered at $T > 450$ K. The ratio of LT and HT signals depends on particle size: smaller particles lead to a larger fraction of terminally bonded CO and thus to a larger amplitude for the LT peak [3].

Therefore, the TPD spectra presented in figure 4 provide strong evidence for carbon species inhibiting CO adsorption in highly coordinated sites.

For larger particles, mainly exposing (111) facets, the adsorption capacity toward CO decreases with increasing amount of carbon deposited, as shown in the inset in figure 4(b). This result is in line with those obtained for CO adsorption on the ethylidyne pre-covered Pd.

Particles supported on Al_2O_3 powder [14], and on mica [15]* as well as for CO on the ethylidyne pre-covered Pd(111) single crystal surface [16].

For smaller particles, the CO desorption signal area turns out to be independent of carbon deposits (see the inset in figure 4(a)), but the shape of the desorption signal is drastically changed. It shows that carbon deposition re-distributes the population of CO adsorption sites by pushing CO to adsorb on the more weakly bound on-top sites as the highly coordinated sites are occupied by carbon species.

One question which might be addressed here is whether carbon deposition proceeds homogeneously on the surface or via a spatial "islanding" as has been directly observed by STM on the Pt(111) single crystal surface [17]. It should be mentioned that Pt exhibits a much higher dehydrogenation ability as compared with Pd, and to our knowledge, there are no STM data for Pd surfaces so far. Note that in the case of formation of carbon islands with C–C bonds we would expect the CO desorption features to decrease simultaneously. However, we have actually observed the preferential vanishing of the HT peak, which originates from multiply coordinated sites.

*In their study [15], the authors performed CO adsorption/desorption measurements starting from 333 K, thus monitoring only the HT desorption state. This might be the reason why smaller particles (~2 nm) caused a larger CO peak area loss as compared with the largest particles (~14 nm), since low-temperature states (linear CO) were not monitored.

3.4. Hydrogen adsorption on carbon-covered Pd

In the present study, we performed D_2 adsorption at ~200 K. This temperature is close to the onset of the H_2 (D_2) TPD signals observed on many Pd single crystal surfaces at relatively low exposures [18,19].

Figure 5 shows D_2 TPD spectra for the clean and carbon-covered Pd surfaces. Three adsorption states can be distinguished for the clean surface, centred at about 230, 290 and 340 K and denoted as β_0, β_1 and β_2, respectively. The position of the peaks and their

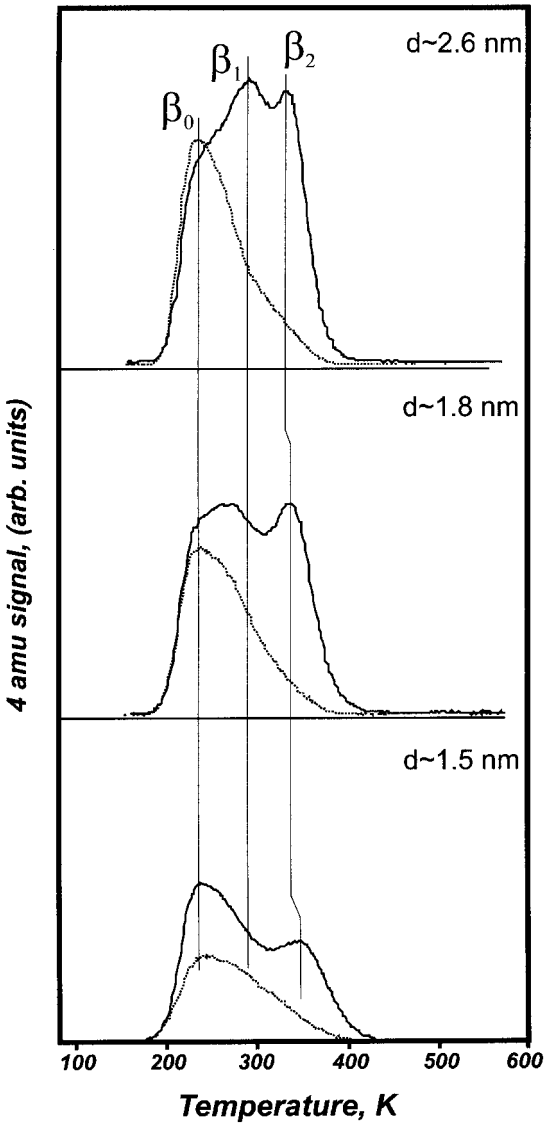

Figure 5. D_2 TPD spectra (1.5 L of D_2 at 195 K) for the clean (—) and carbon-covered (···) Pd particles of different sizes as indicated. Carbon was deposited by two ethene TPD cycles.

dependence on particle size are quite similar to those observed for the pristine $Pd/Al_2O_3/NiAl(110)$ system [6]. The β_2 state has previously been assigned to H (D) atoms adsorbed on the surface. Regarding the β_0 and β_1 states, it is difficult to make a definitive assignment; however, according to literature data obtained for different Pd single crystal surfaces, we have attributed them to the presence of sub-surface hydrogen [6].

Comparing the D_2 TPD spectra, we see that formation of the β_2 state (*i.e.* surface D atoms) is strongly inhibited by the presence of carbon species. Since the H (D) ad-atoms are known to occupy the hollow sites on the clean Pd surfaces [19], this fact supports the above conclusion that carbon species in fact reside in the hollow sites.

On the other hand, the effect of carbon on the β_0 desorption state is negligible, at least for the large (2.6 nm) particles. It becomes stronger as the particle size decreases. The effect on the β_1 state seems to exhibit an intermediate behavior between the β_2 and β_0 states.

It appears that H_2 (D_2) dissociation is still possible on carbon-covered surfaces since it occurs on the on-top sites of Pd [19]. However, the H (D) ad-atoms formed cannot remain on a surface blocked by carbon species and must migrate into the sub-surface region.

3.5. *Effect on ethene hydrogenation on Pd*

As mentioned in the introduction, we have recently studied the ethene hydrogenation reaction on the pristine $Pd/Al_2O_3/NiAl(110)$ system [6]. That study revealed that, on low-temperature adsorption of ethene on hydrogen pre-covered Pd particles, ethane is formed which desorbs at ~200 K on heating.

It has been found that ethane production is much higher in the presence of sub-surface hydrogen. This might indicate that either ethene directly reacts with sub-surface hydrogen or it reacts with hydrogen on the surface but the latter reaction is promoted by sub-surface hydrogen.

In addition, the desorption temperature of ethane formed during a TPD run correlates with the adsorption temperature of hydrogen. This means that ethane desorption is reaction limited, *i.e.* ethane desorbs immediately after it is formed by the reaction of ethene with the most weakly bound hydrogen present. In other words, there must be overlap of π-bonded ethene and sub-surface hydrogen adsorption states for the reaction to occur as schematically depicted in figure 6.

For studying particle size effects on the hydrogenation reaction, we measured the integral amount of ethane formed during a TPD run for co-adsorbed 1 L of D_2 at 200 K and then 1 L of C_2D_4 at 90 K. This amount was normalized to the Pd surface area calculated on the basis of our structural results for this system. The catalytic activity of Pd, determined in such a manner, has turned out to be independent of particle size in the 1–3 nm range under the conditions studied [6].

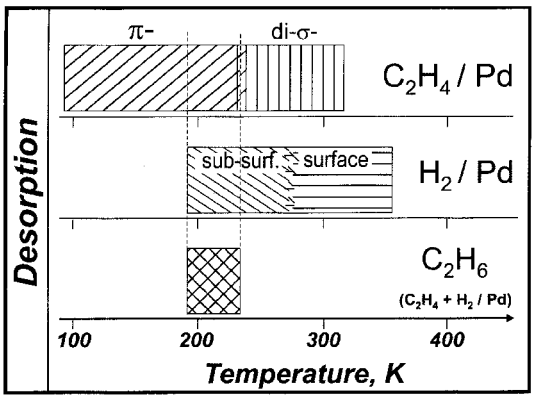

Figure 6. The scheme illustrates the model of overlapping adsorption states of π-bonded ethene and sub-surface hydrogen for the hydrogenation reaction to occur in the co-adsorption experiments on a pristine $Pd/Al_2O_3/NiAl(110)$ system [6].

In order to reveal the effects of carbon deposits on the reaction, we have performed similar co-adsorption experiments and compared the amounts of ethane produced in the first (*i.e.* on the clean surface) and second (*i.e.* on the carbon-modified surface) TPD runs. Figure 7 presents the corresponding ratios of ethane production for the different particle size.

The results show that hydrogenation is strongly inhibited by carbon species. The ethane production drops by a factor of 2–3 almost independently of particle size. In order to explain such an effect, we have to recall how carbon deposits influence the ethene and hydrogen adsorption as discussed in the previous sections.

Firstly, π-bonded ethene, which is assumed to be the reactive species in the hydrogenation reaction [6,11,20], is not influenced much by carbon deposits (see figure 1). However, the dehydrogenation route for di-σ-bonded ethene is suppressed by carbon. Therefore, the activity

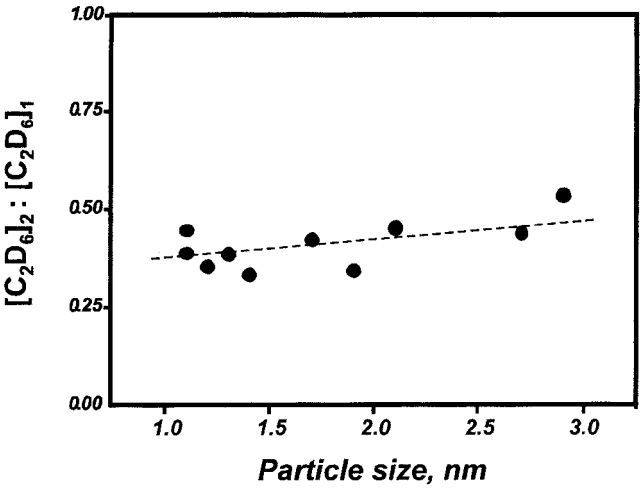

Figure 7. Ratio of integral amounts of ethane produced during second ($[C_2D_6]_2$) and first ($[C_2D_6]_1$) TPD runs for co-adsorbed 1 L of D_2 at 200 K and 1 L of C_2D_4 at 100 K as a function of particle size.

could increase if, for example, di-σ-bonded ethene were involved in the hydrogenation reaction.

Regarding the effect on hydrogen, the data have revealed that the *total* amounts of D_2 adsorbed on the post-reacted samples are decreased by a factor of $\sim$2 (not shown here, but the spectra are quite similar to those observed after ethene adsorption only, as presented in figure 5). This correlation between hydrogen adsorption capacity and ethane production indicates that the drop in activity obtained for carbon-covered Pd particles can be attributed to a lower hydrogen coverage on Pd, in agreement with first-order reaction kinetics with respect to hydrogen as observed on this system [20] and the Pd/Al_2O_3 catalyst [21] at high-pressure conditions.

However, if we look at the effect of carbon on the hydrogen adsorption into the different states, we find that sub-surface ($\beta_0 + \beta_1$) states are less affected as compared with the β_2 state attributed to H (D) ad-atoms residing on the surface (figure 5). Therefore, according to the model of overlapping states depicted in figure 6, if sub-surface hydrogen were directly involved in the reaction with π-bonded ethene, one would expect hydrogenation activity to be only slightly influenced by the presence of carbon species. However, this is not the case even for the 2.6 nm particles, for which the observed changes for the β_0 state are negligible (see figure 5).

It therefore appears that π-bonded ethene in fact reacts with surface hydrogen atoms, which are repopulated from the reservoir in the sub-surface region. Therefore, the activity for carbon-covered Pd particles is significantly smaller simply because of the lower number of sites available for hydrogen ad-atoms.

Also, one should consider the possible steric effects of carbonaceous species on the hydrogen addition to C_2H_4 and C_2H_5 species on the surface.

Certainly, further experiments employing IRAS and other spectroscopy techniques should be done to elucidate the reaction mechanism on these model systems.

4. Summary and conclusions

In the present paper, we have performed a TPD study of ethene, CO and hydrogen adsorption and co-adsorption on Pd particles, deposited on a thin alumina film, in the presence of carbon deposits. Carbon species were formed by ethene dehydrogenation on heating to $\sim$550 K. The results can be summarized as follows.

1. Ethene adsorbs on Pd in a π- or a di-σ-bonded state. π-bonded ethene desorbs intact at $T < 250$ K independently of the carbon deposits. Di-σ-bonded ethene can either desorb at $\sim$330 K or dehydrogenate. Carbon species do not prevent di-σ-ethene *adsorption*, but inhibit its *dehydrogenation* upon heating.
2. The desorption temperature for CO on Pd shifts to lower temperatures by 50–100 K, thus indicating that, on average, CO is more weakly bound in the presence of the carbon species. This effect depends on particle size, and it is stronger for the smallest particles.
3. Carbon deposits suppress formation of surface hydrogen. The influence on sub-surface hydrogen is comparatively weak, but depends on the particle size. Again, the effect is stronger for the smallest particles.

The above-mentioned effects can be rationalized by the fact that carbon species prefer a high coordination with Pd surface atoms and thus occupy, for example, 3-fold hollow sites. Thus, it can be logically argued that the carbon species: (1) inhibit ethene dehydrogenation; (2) push CO molecule to on-top sites, and (3) hydrogen into sub-surface sites.

Finally, the ethene hydrogenation reaction is suppressed by carbon deposits. We rationalize this in terms of the site-blocking effect on hydrogen adsorption as indicated in (3).

Acknowledgments

The authors thank M. Naschitzki for technical support. Financial support by the following agencies is gratefully acknowledged: Deutsche Forschungsgemeinschaft (DFG), Bundesministerium für Bildung und Forschung (BMBF) and Fonds der Chemischen Industrie. Synetix, a member of the ICI group, has supported this work through the ICI Strategic Research Fund. J.C.H. thanks the Alexander-von-Humboldt Foundation for a senior scientist award.

References

[1] G. Webb, Catal. Today 7 (1990) 139.
[2] M. Bäumer and H.-J. Freund, Prog. Surf. Sci. 61 (1999), 127.
[3] M. Frank and M. Bäumer, Phys. Chem. Chem. Phys. 2 (2000) 3723.
[4] J. Meusel, J. Hoffmann, M. Hartmann, M. Heemeier, M. Bäumer, J. Libuda and H.-J. Freund, Catal. Lett. 71 (2001) 5.
[5] M. Frank, M. Bäumer, R. Kühnemuth and H.-J. Freund, J. Vac. Sci. Technol. A 19 (2001) 1497.
[6] Sh. Shaikhutdinov, M. Heemeier, M. Bäumer, T. Lear, D. Lennon, R.J. Oldman, S.D. Jackson and H.-J. Freund, J. Catal. 200 (2001) 330.
[7] Sh. Shaikhutdinov, M. Heemeier, J. Hoffmann, I. Meusel, B. Richter, M. Bäumer, J. Libuda, H. Kuhlenbeck, H.-J. Freund, R.J. Oldman, S.D. Jackson, C. Konvicka, M. Schmid and P. Varga, submitted to Surf. Sci.
[8] J.A. Gates and L.L. Kesmodel, Surf. Sci. 124 (1983) 68.
[9] M. Nishijima, J. Yoshinobu, T. Sekitani and M. Onchi, J. Chem. Phys. 90 (1983) 5114.
[10] E.M. Stuve, R.J. Madix and C.R. Brundle, Surf. Sci. 152/153 (1985) 532.
[11] N. Sheppard and C. De La Cruz, Adv. Catal. 42 (1998) 181.
[12] C. Klink, F. Besenbacher, I. Stensgaard and E. Laegsgaard, Surf. Sci. 342 (1995) 250.
[13] I.S. Tilinin, M.K. Rose, J.C. Dunphy, M. Salmeron and M.A. van Hove, Surf. Sci. 418 (1998) 511.

[14] T. Beebe Jr. and J.T. Yates Jr., Surf. Sci. Lett. 173 (1986) L606.
[15] W.G. Durrer, H. Poppa, J.T. Dickinson and C. Park, J. Vac. Sci. Technol. A3 (1985) 1545.
[16] D. Stacchiola, M. Kaltchev, G. Wu and W.T. Tysoe, Surf. Sci. 470 (2000) L32.
[17] T.A. Land, T. Michely, R.J. Behm, J.C. Hemminger and G. Comsa, J. Chem. Phys. 97 (1992) 6774.
[18] G. Gdowski, T. Felter and R. Stulen, Surf. Sci. 181 (1987) L147.
[19] K. Christmann, Surf. Sci. Rep. 9 (1988) 1.
[20] G. Rupprechter, H. Unterhalt, M. Morkel, P. Galletto, L. Hu and H.-J. Freund, Surf. Sci. (2001) in press.
[21] T. Beebe Jr. and J.T. Yates Jr., J. Am. Chem. Soc. 108 (1986) 663.